

# Continuous point-like high-temperature laser discharge produced by terahertz free electron laser

Cite as: AIP Advances 7, 095123 (2017); <https://doi.org/10.1063/1.4992058>

Submitted: 26 June 2017 • Accepted: 14 September 2017 • Published Online: 25 September 2017

V. V. Kubarev, Ya. V. Getmanov and O. A. Shevchenko



View Online



Export Citation



CrossMark

## ARTICLES YOU MAY BE INTERESTED IN

[A point-like source of extreme ultraviolet radiation based on a discharge in a non-uniform gas flow, sustained by powerful gyrotron radiation of terahertz frequency band](#)

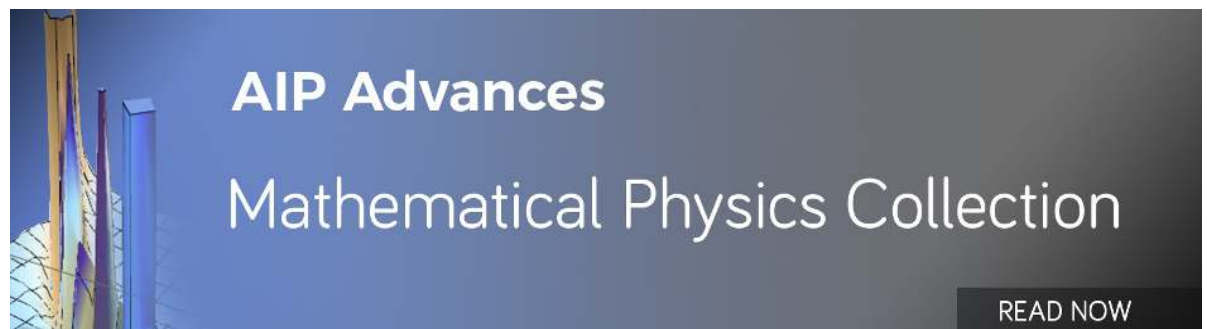
Applied Physics Letters **105**, 174101 (2014); <https://doi.org/10.1063/1.4900751>

[Nanoscale piezoelectric vibration energy harvester design](#)

AIP Advances **7**, 095122 (2017); <https://doi.org/10.1063/1.4994577>

[Numerical treatment of Hunter Saxton equation using cubic trigonometric B-spline collocation method](#)

AIP Advances **7**, 095124 (2017); <https://doi.org/10.1063/1.4996740>



## Continuous point-like high-temperature laser discharge produced by terahertz free electron laser

V. V. Kubarev,<sup>1,2,a</sup> Ya. V. Getmanov,<sup>1</sup> and O. A. Shevchenko<sup>1</sup>

<sup>1</sup>*Budker Institute of Nuclear Physics, Lavrentiev Av. 11, 630090 Novosibirsk, Russian Federation*

<sup>2</sup>*Novosibirsk State University, Pirogova St. 2, 630090 Novosibirsk, Russian Federation*

(Received 26 June 2017; accepted 14 September 2017; published online 25 September 2017; publisher error corrected 28 September 2017)

A continuous point-like laser discharge of record high temperature has been produced in argon at atmospheric pressure with focusing of the radiation of the Novosibirsk terahertz free electron laser (NovoFEL). According to spectral measurements, the temperature in the center of the millimeter-sized plasma sphere was 28000 K at a plasma density of  $1.5 \times 10^{17} \text{ cm}^{-3}$  and an average NovoFEL power of 200 W at a wavelength of 130  $\mu\text{m}$  (2.3 THz). © 2017 Author(s). All article content, except where otherwise noted, is licensed under a Creative Commons Attribution (CC BY) license (<http://creativecommons.org/licenses/by/4.0/>). <https://doi.org/10.1063/1.4992058>

### I. INTRODUCTION

The laser optical discharge is a specific type of gas discharge with a temperature 2-3 times higher than that in other discharges, which makes it of great interest both for fundamental science and many practical applications.<sup>1</sup> The pulsed laser discharge was first obtained in the optical range using a Q-switched ruby laser.<sup>2</sup> The appearance of high-power infrared CO<sub>2</sub> lasers launched intense study of the continuous laser optical discharge.<sup>1</sup> Currently, the applications of the laser discharge are very diverse. These are various laser-plasma technologies for surface modification and creation of various coatings, as well as non-contact laser switching in high-voltage systems. The creation of high-power microwave and terahertz sources enabled experiments with the discharge in the long-wave part of the spectrum. The use of the laser or microwave discharge together with ablation allows obtaining new materials, such as nanopowders,<sup>3</sup> nano-tubes<sup>4</sup> and nano-horns.<sup>5</sup> Rectification of femtosecond optical laser pulses by means of the gas laser discharge is now used for generation of pulsed terahertz radiation.<sup>6-12</sup>

The continuous point-like high-temperature laser discharge is very useful in spectroscopy as a source of broad-band radiation and as plasma medium for excitation of multicharged ions. The point-like laser discharge created by lasers of optical range in medium of high-pressure inert gases allowed cardinally improving the brightness, spectral range, stability, and life-time of spectroscopic radiation sources. The modern light sources referred to as LDLs (laser driven light source) have unique parameters due to the high laser discharge temperature (estimated as 10000-20000 K, which is significantly higher than the 5000-7000 K typically achieved in a short-arc Xe lamp).<sup>13</sup> Now the sources are commercially available.<sup>14</sup>

Analytical spectroscopy is based in particular on handbook experimental data for atomic and ionic lines. The intensities of the lines of multicharged ions are very weak in arc-plasma because the temperature of the medium is much less than the excitation potentials of the lines. It will also be illustrated in the paper. Thus, increasing the temperature both of light sources and of active excitation sources is a topical problem of modern spectroscopy.

The point-like high-temperature optical discharge is considered to be a promising source of radiation in UltraViolet Lithography (UVL) and Extreme-UltraViolet Lithography (EUVL).<sup>15-18</sup>

---

<sup>a</sup>Author to whom correspondence should be addressed: [V.V.Kubarev@inp.nsk.su](mailto:V.V.Kubarev@inp.nsk.su)



Generation of intense and bright ultraviolet radiation requires a high-temperature point-like discharge. Occurrence of discharge at atmospheric pressure and maximal energy efficiency are desirable for industrial applications.

The study of optical discharge on NovoFEL is motivated by the fact that the laser is a user facility. The high-temperature terahertz optical discharge is planned to be used in many experiments in the field of gas-plasma dynamics, nonlinear harmonic generation, creation of nanomaterials and others.

One of the main physical difficulties in the problem of creation of high-temperature optical discharge is the absorption of laser or microwave radiation by the discharge plasma. In the short-wave optical range, this absorption is very small, and thus effective discharges can be obtained at pressures of tens and hundreds of atmospheres. With increasing the wavelength  $\lambda$ , the absorption coefficient grows as  $\lambda^2$ , yet remaining rather small ( $\sim 1 \text{ cm}^{-1}$ ) even in the infrared range of CO<sub>2</sub> lasers.<sup>1</sup> This means that effective discharges at this wavelength must have a sufficiently large size ( $\sim 1 \text{ cm}$ ), which is confirmed in practice.<sup>1</sup> The largest discharge temperatures of 21000 K and 22000 K were attained in hydrogen and in nitrogen at 6 atm and 2 atm, respectively (see Ref. 1). A temperature of 18000 K was observed in argon at 2 atm. In air, a discharge temperature of 17000 K was measured at 1 atm with the use of a 6-kW CO<sub>2</sub> laser.<sup>19</sup>

An opposite situation is observed in the case of microwave radiation. Even a low-pressure plasma effectively absorbs this radiation, whereas creation of dense plasma is impossible because of the rather low critical plasma density at which radiation is reflected from the plasma. For this reason, microwave experiments are conducted in vacuum chambers, the gas supplied locally to the discharge region.<sup>18</sup> All this, obviously, greatly complicates the possible technological setups.

In this paper we describe a millimeter-sized laser discharge at atmospheric pressure in the terahertz range, which is optimal for such discharge parameters. Due to this, the discharge has a record high temperature and good efficiency.

## II. EXPERIMENTAL SETUP AND METHODS

The source of radiation in the experiments was the Novosibirsk Free Electron Laser (NovoFEL), which is currently the most powerful source of terahertz radiation in the world<sup>20</sup> and the only source capable of maintaining a continuous terahertz laser discharge. The terahertz NovoFEL was generating a continuous sequence of 70-ps (FWHM) pulses with a repetition rate of 5.6 MHz at a wavelength of 130  $\mu\text{m}$  (2.3 THz frequency). The average radiation power in this experiment was 200 W; the peak pulse power was 0.5 MW. The input NovoFEL radiation beam in the experimental setup was close to an ideal Gaussian beam with a width of 22 mm (FWHM). When a parabolic mirror with a relative aperture of 1:1 (Fig. 1) focused this beam, there appeared a Gaussian beam waist of a 0.15 mm (FWHM), the radiation intensity on the axis of the focal spot being equal to 1.6 GW/cm<sup>2</sup>.<sup>21</sup> All our experiments were carried out at atmospheric pressure. Various gases were fed through a tube (Fig. 1) to the radiation focusing area, where they completely displaced the atmospheric air. The gas system had an important feature of a medical needle on the gas tube end. It allowed creating of a localized point-like discharge for a certain optimal gas flow and an optimal geometrical position of the needle. According to Ref. 21, a laser breakdown of atmospheric gases was observed at radiation intensities in the range of 1.1-1.6 GW/cm<sup>2</sup>. A principal difference of argon, which has a minimum breakdown threshold of 1.1 GW/cm<sup>2</sup>, from other gases (helium, air, nitrogen, or carbon dioxide) was the transformation of the discharge breakdown stage with a minimum plasma content into an intense laser-plasma discharge, in which the plasma volume and the optical radiation intensity were much larger, at a NovoFEL power exceeding the threshold breakdown values by 30-50%.<sup>21</sup> In the case of air, nitrogen or carbon dioxide, no such transition was observed even at powers twice the threshold value. In the conditions of our experiment, the radiation of the gas discharges had form of a train of separate pulses, without the equilibrium plasma stage.<sup>22</sup> In the case of helium, an intermediate situation was observed, with a relatively large volume of plasma appearing of much lower brightness and temperature than of argon plasma. In what follows we will consider only the most effective argon laser-plasma discharge.

Two significant effects of the radiation-plasma interaction were observed. As is well known, radiation with a frequency below the critical plasma frequency  $\omega_p[s^{-1}] = 5.65 \times 10^4 \times n_e^{1/2} [\text{cm}^{-3}]$ ,

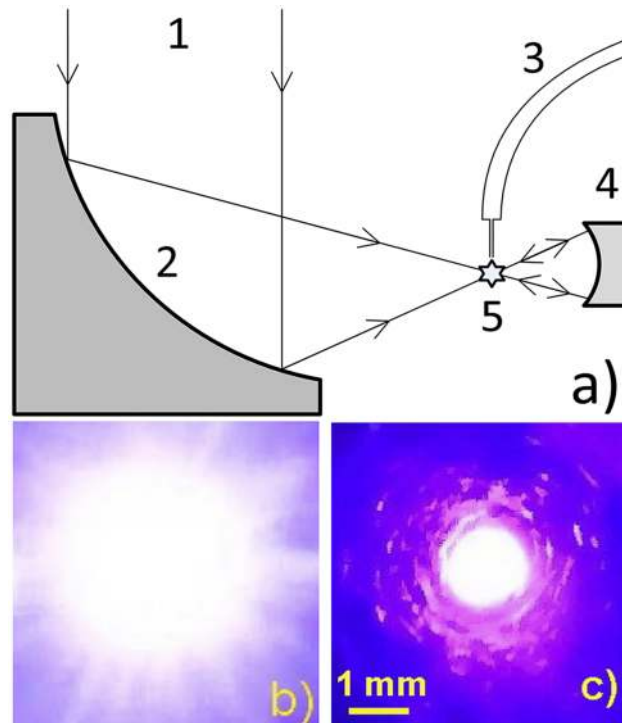


FIG. 1. Optical scheme of experiment (a) and photos of high-temperature point-like laser discharge without (b) and with (c) navy-blue glass filter: 1 – Gaussian-like NovoFEL terahertz beam, 2 – 60 mm off axis parabolic focusing mirror with focal length of 50 mm, 3 – gas tube with medical needle on end, 4 – 20 mm stabilizing spherical mirror with focal length of 20 mm, 5 – laser discharge. Exposition time of the photos: a few milliseconds.

where  $n_e$  is the plasma density, does not penetrate into the plasma. A plasma with a density exceeding the critical value ( $7 \cdot 10^{16} \text{ cm}^{-3}$  for a frequency of 2.3 THz) easily arises in an argon discharge.<sup>22</sup> Therefore, it is usual that an argon plasma discharge has auto-oscillations at the sonic or sub-megahertz frequencies. The arising plasma of the critical density expands and causes shielding of the central area of radiation focusing, which is optimal for maintaining the discharge. Because of this, the discharge decays, but it appears again after relaxation of the plasma. The rate of this relaxation in typical cases is defined by diffusion, which causes self-oscillations at a low sonic frequency.<sup>23</sup> At a higher laser power, we have observed a faster plasma relaxation; this relaxation resulted in self-oscillations at sub-megahertz frequencies.<sup>23</sup> When an additional spherical mirror was placed behind the plasma and reversed the radiation passing through the plasma (at the moment of its decay) back to the plasma, a negative feedback was realized, which completely stabilized these self-oscillations. Experiments on discharge stabilization will be described in detail in a separate publication.

The plasma shielding also has another effect, decrease in the plasma temperature as the plasma volume increases. In our experiments we usually observed a plasma discharge in the form of an almost symmetrical ball (Fig. 1c). It is clear that at an approximately equal power of plasma heating by the laser, a smaller plasma ball will have a higher temperature, due to the higher density of laser energy arriving at the plasma. Thus, to obtain a high plasma discharge temperature it is necessary to moderately restrict the volume of the produced plasma. In our experiments this was done in two ways. The first way was reducing the flow of argon, which displaced the air, so that the optimum purely argon atmosphere was created only near the focus. The second method, which allows obtaining a more stable discharge, consisted in localized gas supply exactly to the focusing area by means of the medical needle at the end of the gas tube (Fig. 1a). The criterion for high-temperature plasma creation was the form of the spectra of optical emission from the plasma, which were continuously observed in the range of 300-1050 nm with the help of a compact spectrometer Mightex-HSR-BD1-005. These spectra are described in detail below. Here we only note that the continuum spectrum of the high-temperature point discharge shifted toward the short waves and, most importantly, there

appeared intense lines of emission of argon ions, which were practically absent in the radiation of the large-volume plasma ball with a diameter of 4-5 mm.

The discharge dynamics was watched in the terahertz radiation using ultrafast detectors on Schottky diodes<sup>24,25</sup> and in the optical radiation using the photodiodes UPD-500-UP and UPD-30-VSG-P made by Alphalas Co.

### III. EXPERIMENTAL RESULTS AND MODEL CALCULATIONS

Parameters of the discharge under investigation were determined mainly from spectroscopic measurements. Figure 2 shows a typical spectrum at the output of the spectrometer. It can be seen that the discharge emission spectrum consists of a continuum and a set of spectral lines. At parameters typical of plasma laser discharges, a decisive contribution to the continuum is provided by the recombination radiation.<sup>1</sup> This is confirmed by the form of the continua in Figs. 2 and 3, in the left-hand parts of which one can clearly see typical recombination bands with a sharp right boundary. In general, the continuum spectrum is similar to solid gray body emission, the shape of whose spectrum can be used for determination of its temperature.<sup>26</sup> In particular, the maximum and center of gravity of our continuum shifts toward the long waves as the size of the plasma ball increases and its temperature decreases. It will be shown below that the main contribution to the discharge radiation comes from regions with very high temperature. On the other hand, in the visible region of the spectrum we observe radiation that is basically given by the external excited levels of argon ions and atoms. In our opinion, in the steady-state regime of our discharge, the numerous close levels of the outer shell of excited particles and plasma electrons can be in an approximate thermodynamic equilibrium, when during recombination into these levels the emission from plasma electrons is balanced by the inverse process of photoionization from these excited levels. Consequently, the emission from the continuum will be similar to the emission of gray (black) body and the temperature of the central part of the discharge can be estimated from the shape of its spectrum. This method works well at moderate discharge temperatures of 10000 – 20000 K. When the temperature increases above 30000 K, the shape of the continuum ceases depending on the temperature because the maximum of the emission spectrum is far beyond the short-wavelength boundary of the spectral sensitivity function of our spectrometer. In particular, the calculated spectrum of black body emission for temperatures  $T \geq 30000$  K has practically the same shape, and this shape is in good agreement with the emission of our continuum. The Planck spectrum of black-body radiation spectrum for a temperature  $T = 30000$  K multiplied by the function of spectral sensitivity of our spectrometer is presented in Fig. 2. Thus, from the shape of the continuum spectrum, the temperature of the central part of our high-temperature discharge is estimated from below by a value of 30000 K.

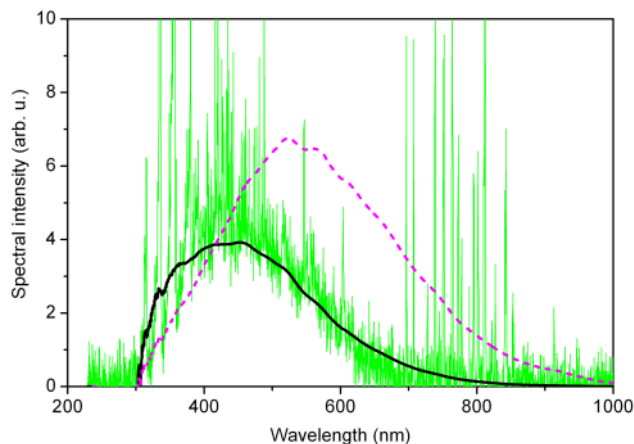


FIG. 2. Experimental spectrum of discharge emission at spectrometer output (curve with peaks); spectral sensitivity of spectrometer (dashed line); calculated spectrum of black body at temperature  $T = 30000$  K multiplied by spectrometer function of spectral sensitivity (smooth solid line).

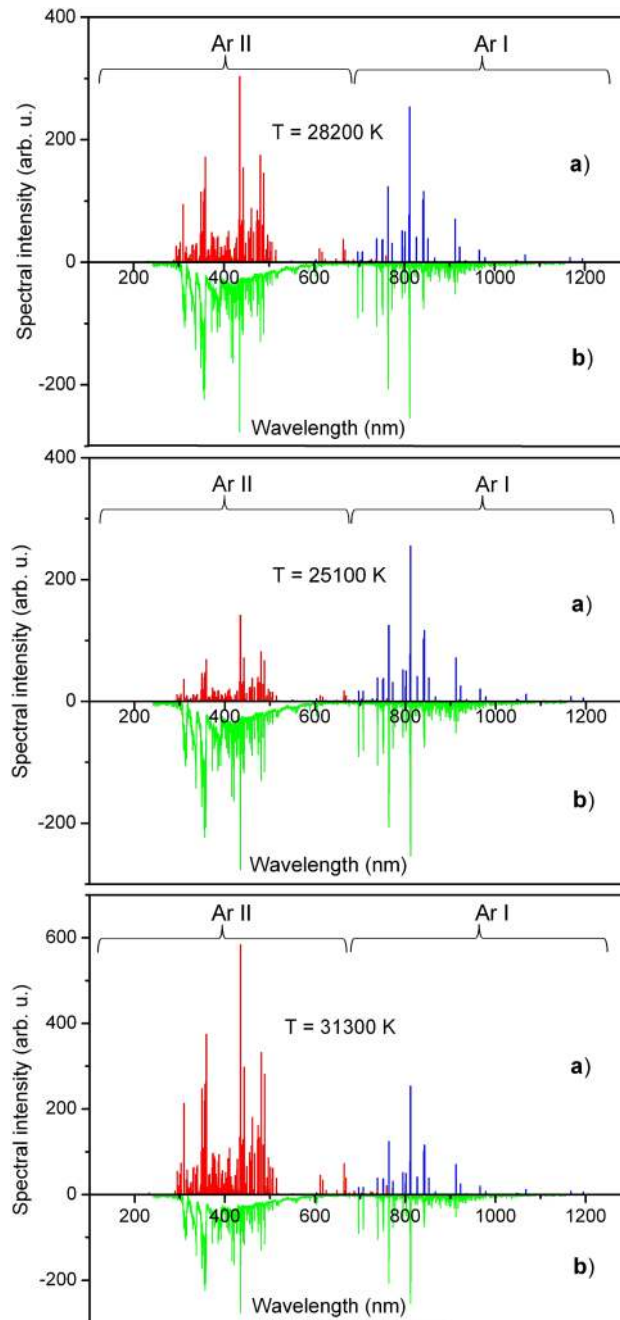


FIG. 3. Comparison of theoretical spectra of high-temperature point laser discharge at different maximum temperatures (a) and experimental spectrum (b): upper spectra:  $T_{\max} = 28200$  K (best coincidence); middle spectra:  $T_{\max} = 25100$  K; lower spectra:  $T_{\max} = 31300$  K; left part of spectra: Ar II ionic lines; right part of spectra: Ar I atomic lines. For convenience of comparison the experimental spectrum is inverted.

More accurate values of the temperature of our high-temperature discharge, which do not contradict the above ones, are obtained from analysis of the intensities of the spectral lines. This discharge has a feature of appearance in the spectrum of lines of singly ionized argon Ar II approximately coinciding in intensity with the atomic lines Ar I.

Detailed analysis of the wavelengths of the lines of the experimental spectrum in Fig. 3 shows that all intense lines with a wavelength shorter than 680 nm are lines of ions Ar II, and those with a wavelength of more than 680 nm are lines of atoms Ar I. The excitation potentials of the



atomic lines ( $\approx 13$  eV) differ significantly from the excitation potentials of the ion lines (19-21 eV). Thus, we have a measurement-friendly strong exponential temperature dependence of the intensity ratio of ionic and atomic lines. In view of this strong dependence, in the theoretical analysis of the line intensities we have to use a model that takes into account the inhomogeneous distribution of the discharge temperature. Previous experiments with laser discharges on CO<sub>2</sub> lasers showed the discharge temperature to monotonically decrease from the center to the periphery.<sup>1</sup> Given the spherical shape of our discharge, we will use the simplest model form of the linear temperature drop, shown in Fig. 4. Our spherical discharge was arbitrarily divided into 10 radial spherical zones with different temperatures; in each zone the plasma and gas densities were found, as well as the intensities of ionic and atomic lines, using the local thermodynamic equilibrium (LTE) model.

The validity of using the LTE model relies on the following assumption. We believe that, although the radiation from the plasma usually forms an appreciable fraction in the energy balance, it does not greatly change the energy distribution of particles in the discharge plasma. The laser radiation energy is transferred to the electron component at the moments of laser pulses, and then their thermalization occurs in a time of  $\sim 1$  ps, followed by establishment of thermal equilibrium between electrons and heavy plasma particles in a time of  $\sim 100$  ns. Analysis of the dynamics of the signals of the spectrum-integrated recombination emission shows that the equilibrium of electrons and heavy particles is established within  $\sim 100$  ns in the intervals between the laser pulses, which follow with a 174-ns period. Thus, on the average, we can assume that our strongly collisional plasma is in thermodynamic equilibrium, with the same average temperature of all particles, which we will regard as the discharge temperature  $T$ . Then the degrees of ionization of the plasma and the population of the levels are completely defined by the Saha-Boltzmann thermodynamic equations.

We calculated these parameters in each radial spherical zone using the open program NIST.<sup>27</sup> As is known, for calculations in the LTE model, in addition to the temperature it is necessary to set the electron density  $n_e$ .<sup>27</sup> We found this density as a parameter at which the same degree of ionization  $\eta$  was obtained from the Saha-Boltzmann equations and from the equality of the discharge pressure to the atmospheric pressure  $P$  in our open system:

$$\eta = n_e / (n_\Sigma - n_e); \quad n_\Sigma = n_e + n_i + n_a = 2n_e + n_a = P/kT, \quad (1)$$

where  $n_i$  and  $n_a$  are concentrations of ions and atoms, and  $k$  is the Boltzmann constant. When comparing the emission of lines from different layers  $j$ , we used a normalization based on the dependence of the line emission intensity  $I_j^{a,i}$  on the plasma parameters  $n_e$  and  $T$ :

$$I_j^{a,i}(n_{a,i}, T) \sim n_{a,i} \times T^{-1} \exp(-\mathcal{E}_j/T), \quad (2)$$

where  $n_{a,i}$  is the density of atoms or ions for the atomic or ionic lines, and  $\mathcal{E}_j$  is the energy of the upper level of the line. The choice of normalization line does not matter much; in our case it was

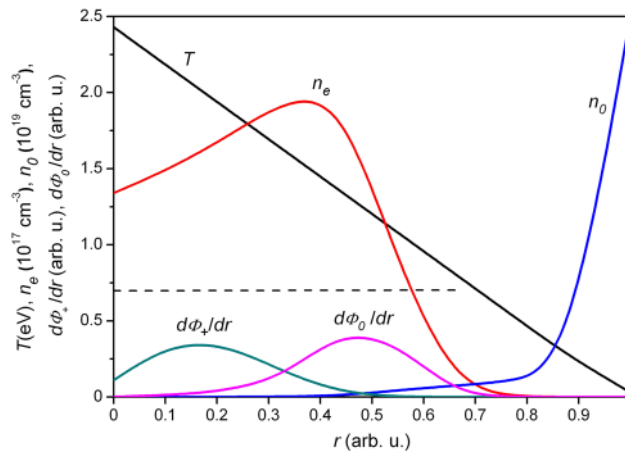


FIG. 4. Radial distributions of temperature  $T$ , plasma and gas densities  $n_e$  and  $n_0$ , and integral radiation of radial spherical layers for ionic  $d\Phi_+/dr$  and atomic  $d\Phi_0/dr$  lines of argon. The dashed line indicates the critical density of the plasma.

the most intense line of ion Ar II (434.8 nm). Emissions from all the zones were summed up with the weights of their volumes because the plasma is transparent for optical radiation and all points of our point discharge are geometrically equivalent for the measurement spectrometer. The only fitting parameter in the criterion of coincidence of the calculation and the experiment was the maximum temperature in the discharge center  $T_{max} = T(r = 0)$ .

Results of the model calculation are shown in the top (a) halves of Fig. 3. The best coincidence of the calculation and experiment is seen for  $T_{max} = 28200$  K. Namely at this temperature the experiment demonstrates an approximate equality of the emission of ionic and atomic lines. At a temperature change by  $\pm 11\%$  only (31300 K and 21100 K), there is seen a two-fold unbalance of these components.

The model calculations also show that in the very center of the discharge (the first zone), the ions are mostly the doubly ionized argon atoms Ar III ( $\sim 60\%$ ). However, at these temperatures the lines of these ions are still too weak to be noticeable against the background of the more powerful recombination and line emission of Ar II.

Figure 4 shows radial distributions of the plasma parameters obtained in the calculation model. In the figure, the maximum temperature  $T_{max} = 28200$  K = 2.4 eV is the best fitting parameter of the line emission calculation presented in Fig. 3. The distributions of plasma and neutral gas densities were also taken from the above line emission calculations for the temperature. One can see the following interesting features. First, it can be seen that the spherical discharge consists of two regions: the area of luminous plasma ( $r < 0.75$ ) and the zone of non-irradiating heated gas ( $0.75 < r < 1$ ). The plasma area is divided into two parts by a critical sphere ( $r_c = 0.59$ ), into which the laser radiation does not penetrate. The main part of plasma radiation is seen to emanate from the sphere with  $r = 0.6-0.65$ . Absorption of laser radiation occurs in plasma layers surrounding this critical sphere from outside, the plasma resonance contributing to the effective absorption of the laser radiation and establishment of high temperature.<sup>18</sup> The experimentally observed spherical shape of our discharge can arise when the center of the plasma is shifted relative to the waist of the focused beam toward the focusing mirror (Fig. 1). We actually observed this shift, although we did not make any special measurements of its value. Note that a plasma density several times exceeding the critical value was observed in the microwave discharge in Ref. 18. In the center of our discharge sphere there is a density dip caused by the temperature increase closer to the center at a constant pressure. The specific integrated radiation of the layers in the ionic lines  $d\Phi_+/dr \sim I_j^i \times r^2$  (the function is almost identical for all most intense ionic lines) is shifted toward the center with respect to the same radiation in the atomic lines  $d\Phi_0/dr \sim I_j^a \times r^2$  (the function is almost identical for all atomic lines). This feature corresponds to the photograph in Fig. 1c), where one can see that the red radiation of the argon atomic lines surrounds the white-color central region, which is a mixture of the red radiation from the atoms of the outer shell and the blue radiation from the ions of the central region.

#### IV. CONCLUSIONS

The Novosibirsk terahertz pulse-periodic free-electron laser is an optimal source for creating a continuous high-temperature point-like laser discharge at atmospheric pressure. A record discharge temperature of  $28000 \pm 1000$  K at a plasma density of  $1.5 \times 10^{17}$  cm<sup>-3</sup> was obtained in argon medium at a relatively small average laser power (200 W) at a wavelength of 130  $\mu$ m (2.3 THz).

#### ACKNOWLEDGMENTS

This work was made with financial support of Russian Foundation for Basic Research (grant 14-22-02070). The NovoFEL operation was supported by Russian Science Foundation (project 14-50-00080).

<sup>1</sup> Yu. P. Raizer, *Gas Discharge Physics* (Springer, 1991).

<sup>2</sup> P. D. Muaker, R. W. Terhune, and C. M. Savage, Proc. 3rd Intern. Quantum Electronics Conference, Paris, 1963.

<sup>3</sup> A. V. Vodopianov, D. A. Mansfeld, A. V. Samohin, N. V. Alekseev, and Yu. V. Tsvetkov, "Production of metallic nanopowders by the method of evaporation-condensation with using focused millimeter radiation at frequency 24 GHz," X Russian workshop on radio physics of millimeter and submillimeter waves," N.Novgorod, Russia, p.129 (2016).



- <sup>4</sup> P. C. Eklund, B. K. Pradhan, U. J. Kim, Q. Xiong, J. E. Fischer, A. D. Friedman, B. C. Holloway, K. Jordan, and M. W. Smith, "Large-scale production of single-walled carbon nanotubes using ultrafast pulses from a free electron laser," *Nano Letters* **2**, 561–566 (2002).
- <sup>5</sup> S. Iijima, M. Yudasaka, R. Yamada, S. Bandow, K. Suenaga, F. Kokai, and K. Takahashi, "Nano-aggregates of single-walled graphitic carbon nano-horns," *Chemical Physics Letters* **309**, 165–170 (1999).
- <sup>6</sup> K. Y. Kim, A. J. Taylor, J. H. Glowina, and G. Rodriguez, "Coherent control of terahertz supercontinuum generation in ultrafast laser–gas interactions," *Nature Photonics* **2**, 605–609 (2008).
- <sup>7</sup> M. K. Chen, J. H. Kim, C. E. Yang, S. S. Yin, R. Hui, and P. Ruffin, "Terahertz generation in multiple laser-induced air plasmas," *Applied Physics Letters* **93**, 231102-(1-2) (2008).
- <sup>8</sup> F. Buccheri and X. C. Zhang, "Terahertz emission from laser-induced microplasma in ambient air," *Optica* **2**, 366–369 (2015).
- <sup>9</sup> B. Clougha, J. Daia, and X. C. Zhang, "Laser air photonics: beyond the terahertz gap," *Materials Today* **15**, 50–58 (2012).
- <sup>10</sup> A. Shkurinov, A. Balakin, A. Borodin, M. Dzhidzhoev, M. Evdokimov, M. Esaulkov, V. Gordienko, and P. Solyankin, "Simultaneous generation of X-ray and terahertz radiation produced by intense femtosecond laser pulses from atomic cluster plasma," *Proceeding of the Int. Conf. IRMMW-THz-2015, Hong Kong, China, M1B-1* (2015).
- <sup>11</sup> Yu. Li and G. Liao, "Studies of powerful terahertz radiation from laser-produced plasmas," *Proceeding of the Int. Conf. IRMMW-THz-2015, Hong Kong, China, H2E-4* (2015).
- <sup>12</sup> K. Liu, D. Papazoglou, A. Koulouklidis, S. Tzortzakis, and X. C. Zhang, "Study of THz emission from ring-airy beam induced plasma," *Proceeding of the Int. Conf. IRMMW-THz-2015, Hong Kong, China, H2E-5* (2015).
- <sup>13</sup> H. Zhu and P. Blackborow, "LDLS sheds light on analytical-sciences applications," *LaserFocusWorld* **47**(12) (2011).
- <sup>14</sup> Energetiq Technology, Inc., "Laser-Driven Light Sources (LDLS™)," <http://www.energetiq.com/contact-energetiq-worldwide-leader-laser-driven-light-sources.php>.
- <sup>15</sup> B. A. M. Hansson, "Laser-plasma sources for extreme-ultraviolet lithograph," Doctoral Thesis, Stockholm, Sweden, 2003.
- <sup>16</sup> O. Sempregz, J. Jonkers, R. Apetz, and M. Yoshioka, "Making extreme-UV light sources a reality," *SPIE Newsroom* (2012).
- <sup>17</sup> H. Mizoguchi, T. Saitoh, and T. Matsunaga, "Development of light sources for lithography at present and for the future," *Komatsu Technical Report* **59**, 1–7 (2013).
- <sup>18</sup> M. Yu. Glyavin, S. V. Golubev, I. V. Izotov, A. G. Litvak, A. G. Luchinin, S. V. Razin, A. V. Sidorov, V. A. Skalyga, and A. V. Vodopyanov, "A point-like source of extreme ultraviolet radiation based on a discharge in a non-uniform gas flow, sustained by powerful gyrotron radiation of terahertz frequency band," *Applied Physics Letters* **105**, 174101 (2014).
- <sup>19</sup> D. R. Keefer, B. B. Henriksen, and W. F. Braerman, "Experimental study of a laser-sustained air plasma," *J. Applied Physics* **46**, 1080–1083 (1975).
- <sup>20</sup> G. N. Kulipanov, E. G. Bagryanskaya, E. N. Chesnokov, Y. Yu Choporova, V. V. Gerasimov, Y. V. Getmanov, S. L. Kiselev, B. A. Knyazev, V. V. Kubarev, S. E. Peltek, V. M. Popik, T. V. Salikova, M. A. Scheglov, S. S. Seredniakov, O. A. Shevchenko, A. N. Skrinsky, S. L. Veber, and N. A. Vinokurov, "Novosibirsk free electron laser—Facility description and recent experiments," *IEEE Transaction on Terahertz Science and Technology* **5**(5), 798–809 (2015).
- <sup>21</sup> V. V. Kubarev, Ya. V. Getmanov, O. A. Shevchenko, and P. V. Koshlyakov, "Threshold conditions for terahertz laser discharge in atmospheric gases," *Journal of Infrared, Millimeter, and Terahertz Waves* **38**(6), 787–798 (2017).
- <sup>22</sup> V. V. Kubarev, "Dynamics of the THz optical discharge," *Proceeding of the Int. Conf. IRMMW-THz-2014, Tucson, USA, T2-A-16.2.* (2014).
- <sup>23</sup> V. V. Kubarev, Ya. V. Getmanov, and O. A. Shevchenko, "Self-oscillations in terahertz laser discharge: Nature, parameters, and suppression," *Proc. 41st International Conference on Infrared, Millimeter, and Terahertz Waves IRMMW-THz 2016, Copenhagen, Denmark* (2016).
- <sup>24</sup> V. V. Kubarev, V. K. Ovchar, and K. S. Palagin, "Ultra-fast terahertz Schottky diode detector," *Proceeding of the Int. Conf. IRMMW-THz-2009, Busan, Korea, 09030439* (2009).
- <sup>25</sup> V. V. Kubarev, G. M. Kazakevich, Y. U. Jeong, and B. J. Lee, "Quasi-optical highly sensitive Schottky-barrier detector for a wide-band FIR FEL," *Nuclear Instruments and Methods, A* **507**, 523–526 (2003).
- <sup>26</sup> V. V. Kubarev, "Features of the Drummond light of calcium oxide," *Optics and Spectroscopy* **106**(2), 242–247 (2009).
- <sup>27</sup> A. Kramida, Yu. Ralchenko, J. Reader, and NIST ASD Team (2015). NIST Atomic Spectra Database (ver. 5.3). [Online]. Available: <http://physics.nist.gov/asd> [2017, April 15]. National Institute of Standards and Technology, Gaithersburg, MD.